1437

APRIL 1978 PPPL-1437
UC-20f

FOKKER-PLANCK/TRANSPORT ANALYSES OF FUSION PLASMAS IN CONTEMPORARY BEAM-DRIVEN TOKAMAKS

BY

A. A. MIRIN, M. G. MCCOY,
J. KILLEEN, M. E. RENSINK,
D. E. SHUMAKER, D. L. JASSBY,
AND D.E. POST

PLASMA PHYSICS LABORATORY

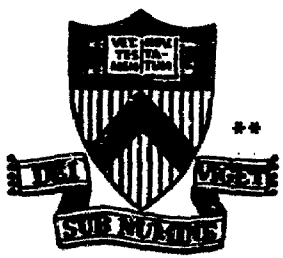

PRINCETON UNIVERSITY
PRINCETON, NEW JERSEY

This work was supported by the U. S. Department of Energy Contract No. EY-76-C-02-3073. Reproduction, translation, publication, use and disposal, in whole or in part, by or for the United States Government is permitted.

FOKKER-PLANCK/TRANSPORT ANALYSES OF FUSION PLASMAS IN CONTEMPORARY BEAM-DRIVEN TOKAMAKS

A. A. Mirin, M. G. McCoy, J. Killeen, M. E. Rensink, D. E. Shumaker
National MFE Computer Center
Lawrence Livermore Laboratory, Livermore, CA 94550, U.S.A.

D. L. Jassby, D. E. Post
Princeton Plasma Physics Laboratory, Princeton, NJ 08540, U.S.A.

ABSTRACT. The properties of deuterium plasmas in experimental tokamaks heated and fueled by intense neutral-beam injection are evaluated with a Fokker-Planck/radial transport code coupled with a Monte Carlo neutrals treatment. Illustrative results are presented for the Poloidal Divertor Experiment at PPPL as a function of beam power and plasma recycling coefficient, R_c. When $P_{beam} = 8$ MW at $E_b = 60$ keV, and $R_c = 0.2$, then $\langle n_{hot}/n_e \rangle \sim 0.5$, $[2/3 \langle E_{ion} \rangle] = 22$ keV $\sim 6 \langle T_e \rangle$, and the D-D neutron intensity is 10^{16} n/sec.

1. INTRODUCTION

In several large tokamak experiments now in operation or under construction, the injected neutral beam power will far exceed the ohmic heating power. By controlling the warm-ion density by gettering or by a magnetic divertor, it is possible to operate in three different reactor-plasma regimes [1]: (1) The energetic-ion regime, where the average ion energy greatly exceeds the electron energy, the plasma recycling coefficient $R_c \ll 1$, $n_{hot}/n_e \geq 0.3$, and the dominant fusion production is by reactions between the energetic ions; (2) The TCT regime, where $n_{hot}/n_e \sim 0.1$, and the dominant fusion production is by beam-target reactions; (3) The beam-driven thermonuclear regime, where $n_{hot}/n_e \ll 0.1$, and the dominant fusion production is by thermonuclear reactions.

For smaller tokamaks with injected powers in the 2 to 12 MW range at 40 to 60 keV, the energetic-ion regime provides the largest neutron intensity [1]. A specific example of the "energetic-ion" regime is the CIT (counterstreaming-ion torus), which is established by beam injection parallel and antiparallel to the magnetic axis [2]. The transition region between the CIT and TCT regimes is perhaps more accessible, and also results in intense fusion-neutron production. In either case the injected beams serve simultaneously to fuel the plasma, to heat electrons and warm ions, and to produce most of the fusion power.

In order to predict and interpret accurately the plasma characteristics and fusion output of intensely beam-driven tokamak plasmas, the time evolution of the velocity-space distribution functions of the energetic species must be calculated using the complete nonlinear Fokker-Planck operator. This paper describes computational studies that make use of the Fokker-Planck/Transport code (FPT) developed at the National Magnetic Fusion Energy Computer Center at Livermore [3]. This code has been integrated with a Monte Carlo neutrals transport treatment [4], a self-consistent beam deposition code [5], and an impurity radiation model [6]. Illustrative results are presented for the Poloidal Divertor Experiment (POX) now nearing completion at PPPL.

2. COMPUTATIONAL MODEL

The FPT Code utilizes an arbitrary number of Maxwellian plasma species which are described by their individual densities $n_a(\rho,t)$ and by a common temperature profile $T_i(\rho,t)$, where ρ is the average radius of a flux surface. The electrons are described by a separately computed temperature profile $T_e(\rho,t)$. An arbitrary number of energetic ion species are represented by distributi. functions of the form $f_h(v,\theta,\rho,t)$, where v is speed and θ is pitch angle.

Neutral beam deposition is computed self-consistently using a Monte Carlo Code [5] that follows fast neutrals from injectors of specified dimensions and focal properties. The injected energetic ions form a hot-ion velocity distribution determined separately for each radial position. The evolution of $f_h(v)$ is described by

$$\frac{\partial f_h}{\partial t} = \left(\frac{\partial f_h}{\partial t}\right)_c + \underset{\text{source}}{\text{beam}} + \text{losses} \qquad (1)$$

The collision operator $(\partial f_h/\partial t)_c$ is that of Rosenbluth, et al [7], where the "Rosenbluth Potentials" g_b and h_b take into account Coulomb collisions among <u>all</u> charged species. The loss terms include charge exchange, fusion burn-up, and transfer to the warm-ion population. The hot ions are assumed to be perfectly confined until they decelerate to an energy $E_{min} = 3/2\ T_e$.

The transport of neutrals in the plasma is determined by a Monte Carlo code [4]. The sources of neutrals include charge-exchange trapping of the injected beams, recycling from the wall, and gas puffing. A Maxwellian warm-ion population is formed from: (i) deceleration of hot ions, (ii) charge-exchange of hot ions, (iii) ionization of warm neutrals formed during neutral-beam trapping, (iv) ionization of neutrals recycled from the wall. The transport equations for the warm ions and electrons are

$$\frac{\partial n_e}{\partial t} = -\frac{1}{\rho}\cdot\frac{\partial}{\partial\rho}(\rho\Gamma_e) + S_{1e} + L_{1e} \qquad (2)$$

$$\frac{\partial}{\partial t}(3/2\ n_e T_e) = -\frac{1}{\rho}\cdot\frac{\partial}{\partial\rho}(\rho Q_e) + S_2 + L_2 \qquad (3)$$

$$\frac{\partial}{\partial t}(3/2\ \sum_i n_i T_i) = -\frac{1}{\rho}\cdot\frac{\partial}{\partial\rho}(\rho Q_i) + S_3 + L_3 \qquad (4)$$

where the transport fluxes are written as linear combinations of the density and temperature gradients and the toroidal electric field. The source (S) and loss (L) terms include phenomena such as beam heating, ion-electron energy transfer, Ohmic heating, radiation loss, ionization and charge exchange. The radiation loss term, which is due to a fixed density of impurity ions, is determined by numerical fits to the curves of Refs. [6]. Although a sophisticated neoclassical transport model may be implemented, the present study uses a simpler model based on empirical transport coefficients:

$$\Gamma_a = D_a\,\partial n_a/\partial\rho \qquad (5)$$

$$Q_e = 5/2\ T_e \sum_a Z_a\Gamma_a + K_e n_e \partial T_e/\partial\rho \qquad (6)$$

$$Q_i = 5/2\ T_i \sum_a \Gamma_a + K_i \sum_a n_a \partial T_i/\partial \rho \qquad (7)$$

The magnitudes and dependences for D, K_i, and K_e are taken to be the same as those observed in present-day tokamak plasmas, such as TFR [8] and PLT [9], namely, $D = 1 \times 10^3[1 + 9(r/a)^2]$ cm2/s, $K_e = (5 \times 10^{17}/n_e)$ cm2/s, $K_i = 1 \times 10^4$ cm2/s. The parabolic D(r) turns out to be roughly equivalent to $D(r) \propto n_e^{-1}$. These transport coefficients are all independent of temperature. At the limiter radius (r = a), we fix $n_h = 0$, $n_e = 3.5 \times 10^{12}$ cm^{-3}, and $T_e = T_i = 0.3$ keV. Neutrals are reflected from the wall with 20 eV energy. For all cases reported herein, an iron impurity with a uniform fixed density of 3×10^{10} cm^{-3} is specified.

Fusion reaction rates are accurately computed via a five-fold velocity-space integral of the fusion cross-section over the reacting distribution functions [10]. Steady-state solutions for all plasma parameters and the fusion-neutron production rate are presented in the following sections.

Table 1. Reference PDX Parameters.

Major radius	1.40 m
Plasma radius	0.42 m
Field at plasma	2.5 T
Plasma current	500 kA
Neutral-beam energy	40 to 60 keV
Neutral-beam power	2 to 12 MW (D°)
	85% at full energy
	15% at half energy
Beam pulse length	1.0 s
Injection angles	50% co-injection
(this study)	50% counter-inj.

4. EFFECT OF RECYCLING COEFFICIENT

The numerical model has been applied to circular plasmas in the PDX device [11] whose principal parameters are given in Table 1. In PDX the recycling coefficient R_c of the plasma can in principal be controlled by the poloidal magnetic divertor. (R_c is defined as the ratio of the rate of cold neutral inflow to the rate of warm-ion outflow.) Figure 1 shows how several important parameters vary with R_c when the D° injection power of 8 MW at 60 keV is held constant. Steady-state solutions are shown. As R_c increases from 0 to 1.0, the relative hot-ion density decreases by a factor of 3, and $\langle \varepsilon_{ion} \rangle$, the average energy of all hot and warm ions, decreases by a factor of 2.4. The fusion power multiplication, Q_p, and neutron intensity decrease by a factor of 3.6. [Here Q_p = (fusion power/injected power), and does not include ohmic heating (~ 0.5 MW).] Additional influx of gas into the plasma from the beam lines would cause a further decrease in Q_p for a given R_c.

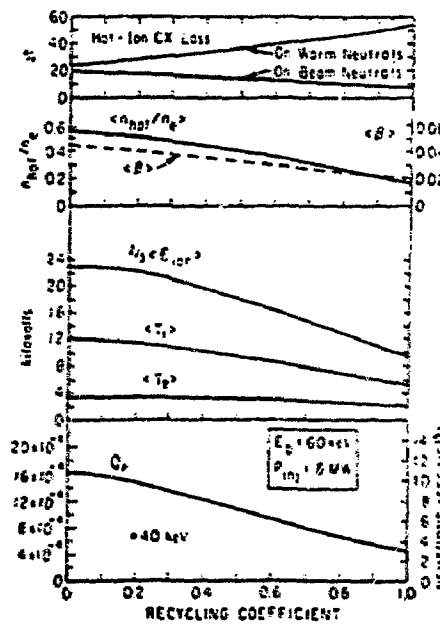

Fig. 1. Variation of spatially-averaged plasma parameters and fusion power gain Q_p with plasma recycling coefficient, for E_b = 60 keV and P_{beam} = 8 MW. (78-3357)

Table 2 gives parameters for the case of R_c = 0.2, where 54% of the fusion power production is due to reactions between the energetic ions, and 40% is due to beam-target reactions. Figure 2 shows the ion velo-

city distribution. Note that Coulomb collisions between ions injected in the same beam cause dispersion to velocities well above the injection velocity.

The accessibility of this CIT/TCT operation requires (1) that $R_c \ll 1$, (2) that the fast ions slow down classically, and (3) that the energetic ions remain close to their magnetic surfaces of birth while slowing down, a time that is of the order of 1.5 times the particle confinement time τ_p. Charge-exchange loss, however, reduces the average hot-ion lifetime.

Table 2. Illustrative Energetic-Ion Regime.

Beam energy	60 keV (D°)
Beam power	8 MW
Recycling coef.	0.20
$n_e(0)$	8.0×10^{13} cm^{-3}
$\langle n_{hot}/n_e \rangle$	0.51
$\langle Z_{eff} \rangle$	1.7 (iron)
$T_e(0)$	5.1 keV
$T_i(0)$	13.9 keV
$2/3 \times \bar{E}_{ion}(0)$	24.6 keV
$n_e(0)\tau_{Ee}$	3.9×10^{12} cm^{-3}s
Hot-ion lifetime	75 ms ~ 1.2 τ_{Ei}
$\langle \beta \rangle$	0.041
Neutron Production (D-D)	
Q_p	1.46×10^{-3}
Thermonuclear	6.1×10^{14} n/s
Beam-Target (TCT)	4.0×10^{15} n/s
Energetic-Ion	5.4×10^{15} n/s
Total intensity	1.0×10^{16} n/s

5. RADIAL PROFILES

Figure 3 shows the radial profiles of various plasma parameters for the cases $R_c = 0.01$ and 0.99. For $R_c = 0.01$, the neutral population at $r < 30$ cm originates mainly from charge-exchange trapping of the neutral beams, while for $R_c = 0.99$, the neutral population is 2 to 3 times larger, and originates mainly by inward diffusion from the plasma boundary. Surprisingly, n_e is nearly the same for the two cases: for $R_c = 0.01$, the hot-ion lifetime is much longer, and these ions are assumed not to undergo radial diffusion; the much larger warm-ion population for $R_c = 0.99$ undergoes relatively rapid diffusion. The average ion energy for $R_c = 0.01$ is about twice that for $R_c = 0.99$, and results in several times higher Q_p (see Fig. 1). The fairly steep density profile but relatively shallow T_e profile are characteristic of plasmes with divertors operating in the "unload" mode.

6. VARIATION WITH BEAM POWER

Figure 4 shows the variation of species temperatures and neutron intensity, F_n, with beam power, when $R_c = 0.20$. It is found that Q_p is nearly proportional to $\langle T_e \rangle$, which increases more rapidly at lower values of P_{beam}. Thus F_n increases as $P_{beam}^{3/2}$ at lower powers, but only linearly with P_{beam} at higher powers. These large neutron production rates are achieved with very small $n_e\tau_{Ee}$, namely 1 to 1.5×10^{12} cm^{-3}s, but with very large average ion energy $\bar{E}_i \sim 25$ to 35 keV. (Here τ_{Ee} is the ratio of the total electron energy to the sum of the rates of electron energy loss by diffusion and radiation; diffusion is dominant.) At higher P_{beam} the predicted beta-values are near the largest that

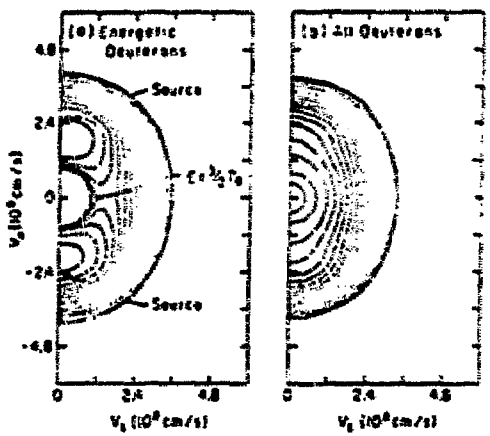

Fig. 2. Steady-state ion velocity distribution in PDX for co- and counter-injection at $E_b = 60$ keV, with $P_{beam} = 8$ MW and $R_c = 0.2$. Energetic ions enter warm Maxwellian at $E = 3/2\ T_e$. (78-3369)

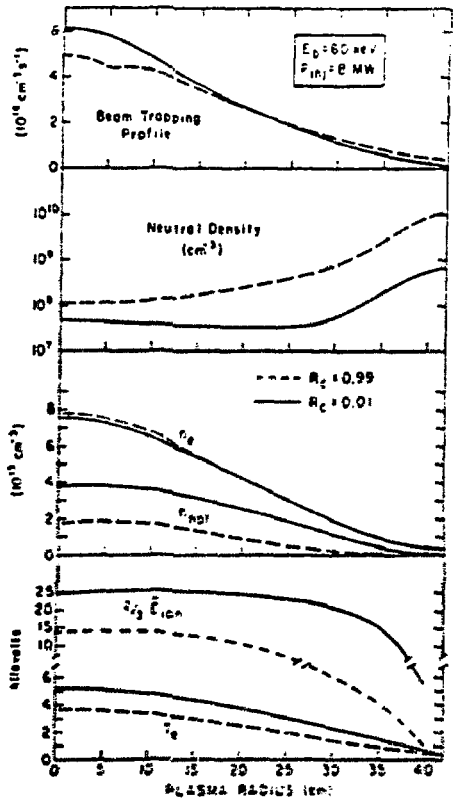

Fig. 3. Radial variation of steady-state plasma parameters for recycling coef. R_c = 0.01 (solid line) and R_c = 0.99 (dashed line). (78-3355)

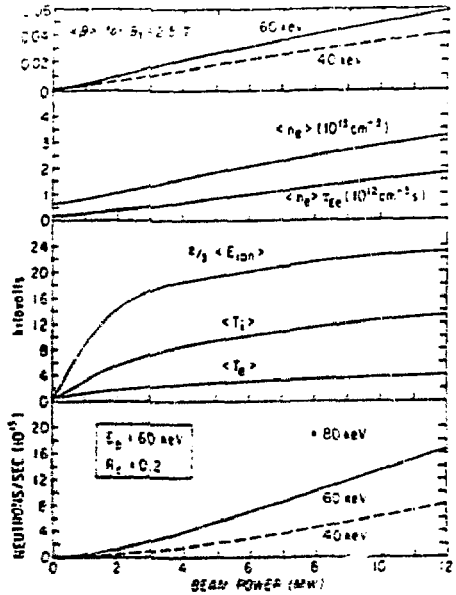

Fig. 4. Variation of spatially-averaged plasma parameters and fusion neutron intensity with beam power, for E_b = 60 keV and recycling coef. = 0.2. $\langle E_{ion} \rangle$ is average energy of all hot and warm ions. Dashed lines are for E_b = 40 keV. (78-3356)

can in theory be sustained in a circular POX plasma. About 85% of the plasma pressure is due to the ions, and 60% is due to the energetic ions alone. The reduced fusion production rate at E_b = 40 keV is due to a smaller beam-target reaction rate and increased charge-exchange loss.

If the bulk plasma temperature could be attained by some means other than by reacting beam injection, F_n would be a factor of 10 to 30 lower. Furthermore, the property $\langle T_i \rangle \sim 3\langle T_e \rangle$ is dependent to a great extent on beam fueling. If $\langle T_i \rangle$ and $\langle T_e \rangle$ were comparable, as expected to be the case with other heating methods, then F_n (and Q_D) would be of the order of 1/100 of the values obtained in beam-driven energetic-ion operation. Finally, we note that parallel-antiparallel injection is not essential for producing large neutron intensities. For example, if approximately half the beams are injected tangentially and half perpendicularly, it is found that the fusion-neutron production is reduced by at most a factor of 1.5. With no opposing counter-injection, it should be possible for the co-injected beams to drive the plasma current [12], with relatively little penalty in neutron production.

7. SUMMARY

Plasmas with average ion energy exceeding 25 keV can be attained in medium-sized tokamak devices (i.e., $B_t a \sim 1$ T-m) with intense neutral-beam injection, provided that plasma recycling is minimized by a magnetic divertor or getter assembly, and that essentially all fueling is performed by the beams. The energetic-ion density is then of the order 0.5 n_e, and the warm-ion temperature is 2 to 3 T_e. In PDX-sized plasmas with 4 to 10 MW of beam injection at E_b = 40 to 60 keV, D-D fusion-neutron intensities in the range 10^{15} to 10^{16} n/s are attainable in this energetic-ion mode of operation. The electron energy confinement time need satisfy only $\langle n_e \rangle \tau_{Ee} \sim 1$ to 2×10^{12} cm^{-3}s.

Initial beam-injection experiments in PLT at the 1-MW level [13] have demonstrated several features of the hot-ion/warm-electron plasmas that our analysis predicts for PDX. When $n_e(0) < 5 \times 10^{13}$ cm^{-3} with 1 MW of 38-keV D° injection, it is reported that $n_{hot}/n_e \geq 0.2$ at the center of the plasma, $T_i > T_e$ and $\bar{E}_i(0) \approx 8$ keV. With co-injection alone, or co- and counter-injection together, the fast-ion slowing-down rate appears to be classical ($\tau_s \sim 0.5\ \tau_o$), with little radial drift of the fast ions [13, 14], thus justifying critical basic assumptions of the present analysis. The largest fusion-neutron intensity is obtained at lower densities, where gas influx and recycling are minimized, and up to 30% of the neutron production is due to reactions between energetic ions [14]. However, neutron intensities of the order of those calculated in this paper will be attainable only by eliminating gas influx entirely, and by minimizing recycling with an effective magnetic divertor or large-area getter pumping system.

Acknowledgment. This work was supported by the United States Department of Energy, Office of Fusion Energy.

References

1. Jassby, D. L., Nucl. Fusion 17 (1977) 309, Sections 1.1, 2, 6.2.
2. Jassby, D. L., in Plasma Physics and Controlled Nuclear Fusion Research (Proc. 6th Int. Conf., Berchtesgaden, 1976) 2, 435; Kulsrud, R. M., Jassby, D. L., Nature 259 (1976) 541; Cordey, J. G., Haas, F. A., Nucl. Fusion 16 (1976) 605.
3. Mirin, A. A., et al., J. Comp. Phys. 23 (1977) 23.
4. Hughes, M. H., Post, D. E., Princeton Report PPPL-1335 (1977).
5. Lister, G. G., Post, D. E., Goldston, R., in Plasma Heating in Toroidal Devices (Proc. 3rd Symp., Varenna, Italy, 1976) 303.
6. Post, D. E., et al., Princeton Report PPPL-1352 (1977).
7. Rosenbluth, M. M., et al., Phys. Rev. 107 (1957) 1.
8. TFR Group, in Theor. and Expt. Aspects of Heating of Toroidal Plasmas (Proc. 3rd Int. Mtg., Grenoble, 1976) 2, 141.
9. PLT Group, in Controlled Fusion and Plasma Physics (Proc. 8th Europ. Conf., Prague, 1977).
10. Cordey, J. G., et al., J. Comp. Phys. (1977).
11. Engin. Problems of Fusion Research (Proc. 6th Symp., San Diego, 1975) 496-523.
12. Singer, C. E., Bromberg, L., Jassby, D. L., in Heating in Toroidal Plasmas (Proc. Int. Symp. Grenoble, 1978).
13. PLT Group, in Plasma Physics and Controlled Nuclear Fusion Research (Proc. 7th Int. Conf., Innsbruck, Austria, 1978), to be published.
14. Strachan, J. D., et al., to be published.